Building a surrogate model of a perfect electric conductor using polynomial chaos expansion and the characteristic mode analysis

Adem YILMAZ[1,2,*] , **Hulusi ACIKGOZ**[1] , **Alaaldeen Barakat Ahmed ELROUBY**[2]

[1]Department of Electrical and Electronics, Faculty of Engineering, KTO Karatay University, Konya, Turkey
[2]Department of Electrical and Electronics, Faculty of Engineering, Ankara Yildirim Beyazit University,
Ankara, Turkey

Abstract: A surrogate model for a perfect electric conductor plate is built by using the polynomial chaos expansion method. The plate is excited via four capacitive coupling elements for which the locations are determined by the analysis of the current distribution for each mode provided by the characteristic mode analysis. A numerical model based on the method of moments is then created to generate a database needed to build the surrogate model. Radiation patterns calculated by the surrogate model are compared with those given by the numerical model. The results show that the surrogate model can mimic the numerical model and it can be used to replace complex numerical models to save computation time and to alleviate the burden on the computation resources. Then, a sensitivity analysis is conducted to exhibit the effect of the parameter deviations on the overall antenna performance and to reveal the influential input parameters. The results of sensitivity analysis are used to reduce the complexity of the overall structure.

Key words: Characteristic mode analysis, polynomial chaos expansion, sensitivity analysis, surrogate model

1. Introduction

Platform-based antennas are designed with a conductive structure and coupling elements that excite the current on the structure. In this kind of antennas, the conductor shape itself is the main radiator since the coupling elements are responsible to excite the desired current distribution on the plate [1, 2]. Platform-based antennas are encountered in daily life, such as shipboard antenna, where the superstructure of the ship is the main radiator with the current excitation accomplished via a monopole antenna [3]; electrically small unmanned aerial vehicle (UAV) antenna, where the body of vehicle is considered a radiator and the coupling elements are located at tail and front-edges of UAV [4]. In platform-based antenna, the desired radiation pattern can be constituted by a set of individual orthogonal pattern that the structure exhibits. The characteristic mode analysis (CMA) is usually applied to obtain the orthogonal patterns, hence to form a desired pattern [5, 6]. The advantage of CMA is that it reveals structure's scattering and radiation properties without any excitation. Hence, it has been widely applied to antenna design, especially platform-based antennas. In this kind of antenna, the ports, a.k.a. coupling elements, provide the excitation of characteristic modes (CMs), which are the real current modes (J_n), on the conductor plate. There are mainly two coupling elements that can be used to excite the CMs on the conducting plate in complex platform antennas: capacitive coupling element (CCE) and inductive coupling element (ICE) [7]. In order to excite the desired current distribution on the conducting plate, the location, phase

*Correspondence: adem.yilmaz@karatay.edu.tr

and magnitude of the coupling elements should be determined carefully. In this work, the CMA is applied to the structure under consideration to specify locations of the coupling elements and to determine their properties. On the other hand, the structure with coupling elements is surrogated with the help of polynomial chaos expansion method to perform a sensitivity analysis.

Sensitivity analysis of the antenna aims to identify the variability of the antenna response due to the variation of each input parameter. For this process, a large number of the designed numerical model should be run with the computer simulation for obtaining a successful statistical analysis. However, this is not feasible when the structure under consideration is computationally expensive. For that reason, a surrogate model, also called metamodel, is built to perform the statistical analysis of the complex antenna structures. Traditionally, Monte Carlo (MC) simulations are used for statistical analysis of the antennas [8]. This technique is based on random selections of the input parameters and on the computation of the corresponding output responses accordingly. Nevertheless, this universal approach may require multitude run of the numerical model to obtain substantial number of samples of the input parameter space in order to obtain high confidence in the desired output response. This may be unmanageable when the structure under consideration is computationally expensive. On the other hand, building a surrogate model is a more efficient method to deal with the complexity of the computational model. There are various types of method that exist in the literature to build a surrogate model successfully, such as polynomial chaos expansion (PCE) [9], artificial neural networks (ANN) [10], Gaussian process Kriging modeling [11], support vector machines (SVM) [12], etc. Among them, PCE has found many applications in different engineering fields due to its effectiveness in modeling complex systems with reasonable number of samples [13–15]. In PCE, a random sampling of each input parameter is given to the computational model and quantities of interest (response of the model) are obtained. Then, within the input and output data at hand, the computational model can be approximated by polynomial series.

In this paper, a platform-based antenna, operating at 1.2 GHz, is considered. The CMA is applied to the structure under consideration to investigate both the current distribution of each mode and the characteristic attributes such as eigenvalues and modal significances. Then, the desired characteristic modes are excited with four CCEs. In order to obtain the surrogate model of the antenna, the sampling of input parameters is performed. The input parameters are the phase and the magnitude of each CCE port. The desired output for each input sample is obtained with the computational model. The input and output data of the computational model are transferred to the PCE to obtain a surrogate model. Then, an error analysis is conducted to ensure the accuracy of the surrogate model. Moreover, a sensitivity analysis is applied to the structure to identify the most important input parameters. Then, the structure is reconsidered with the sensitivity analysis results and the structure is simplified with the most influential input parameters. The comparison between the original structure and the simplified one is presented. This paper is organized as follows: the first section gives the background of the work; Section 2 discusses the CMA and the application of CMA on the considered structure. The location of the proper coupling elements is also discussed in Section 2. A brief introduction to the PCE is presented in Section 3. The surrogate model of the structure is presented in Section 4 and an error analysis is given therein. Lastly, PCE-based sensitivity analysis is demonstrated in Section 5. Finally, the work is concluded with future directions in Section 6.

2. Characteristic mode analysis

The CMA for conducting structures was first introduced by Garbacz [5], and later refined by Harrington and Mautz [6]. The basic idea is to obtain characteristic modes and their associated current distributions, which

is only dependent on the shape and size of the conducting structure. The beauty of the theory came from that there is no need of external excitations to obtain CMs. The results of CMA can be examined with the characteristic attributes, i.e. eigenvalues and modal significance (MS). The latter one is defined in terms of the former one, and the definition can be given as:

$$MS_n = \left| \frac{1}{1 + j\lambda_n} \right| \tag{1}$$

where λ_n is the eigenvalue for the nth mode. The eigenvalue expresses the ratio of reactive power to the real power for the considered mode. Its value can be ranged from minus infinity to plus infinity, and when a specific eigenvalue equals to zero, it indicates that the corresponding mode is the most radiating one for the considered structure. On the other hand, according to (1), the MS can have values between zero and one. If MS value of a mode is close to one, then it is considered to be significant mode and it contributes more to the overall antenna radiation. In this paper, CMA is performed on the rectangular platform, which has dimensions of 150 x 75 mm, between the frequency range of 0.7–1.5 GHz. The results of CMA, such as MS and the surface current distribution, are examined for each mode. Figure 1 shows the first six MS corresponding to six different modes of the structure under consideration. It is observed that mode 1 and mode 2 are the most significant modes for the operating frequency. Hence, these two modes are aimed to be excited in this work since they are the ones that contribute the most to the radiation of the plate.
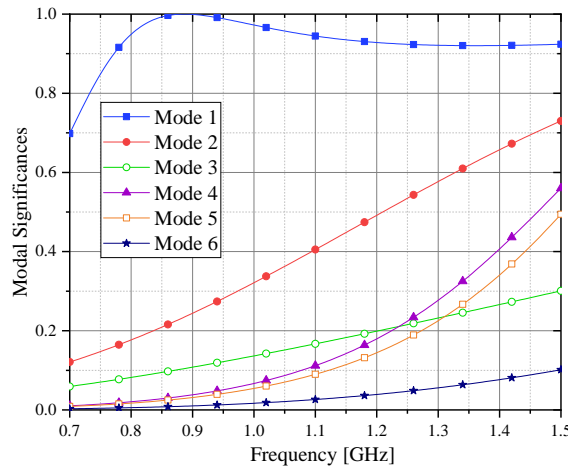

Figure 1. Modal significances vs. frequency of the conducting plate.

In CMA, the total current distribution (J_{tot}) of the structure is given by a set of orthogonal current modes (J_n) (2):

$$J_{tot} = \sum_n a_n J_n \tag{2}$$

where a_n are called modal weighting coefficients (MWC), and they are related to the current modes J_n. J_n are natural current distributions that do not depend on the excitation. On the contrary, MWCs strongly depend on the excitation; thus, the total current distribution on the plate depends on the selective excitation of the modes [7]. In order to excite a certain mode, coupling elements should take place in the platform-based antenna design. Such coupling elements can be either capacitive or inductive, and named capacitive and inductive coupling elements (CCEs and ICEs), respectively. A CCE should be located at a current minimum, and an

ICE should be located at a current maximum. Accordingly, the surface current distribution for each mode is investigated to locate a proper coupling element, and the results are illustrated in Figure 2. It is clear that the current is minimum at each short edge of the plate for mode 1 while it is minimum at each long edge of the plate for mode 2. Since these two modes are the most radiating modes and desired to be excited, the CCEs are placed in the middle of each edge. Overall, the conducting plate is loaded with four CCE ports, and the complete structure can be seen in Figure 3. One can keep in mind that adding the coupling elements do not have a great effect on the characteristic attributes of structure. In order to reveal the effect of adding CCE ports on the conducting plate, the eigenvalues of the structure with and without ports are investigated. It can be seen from Table 1 that adding the CCE ports slightly changes the eigenvalue of mode 1 while it leads mode 2 to be more radiating mode due to the reason that adding ports lead the conducting plate to be appeared electrically larger [16].
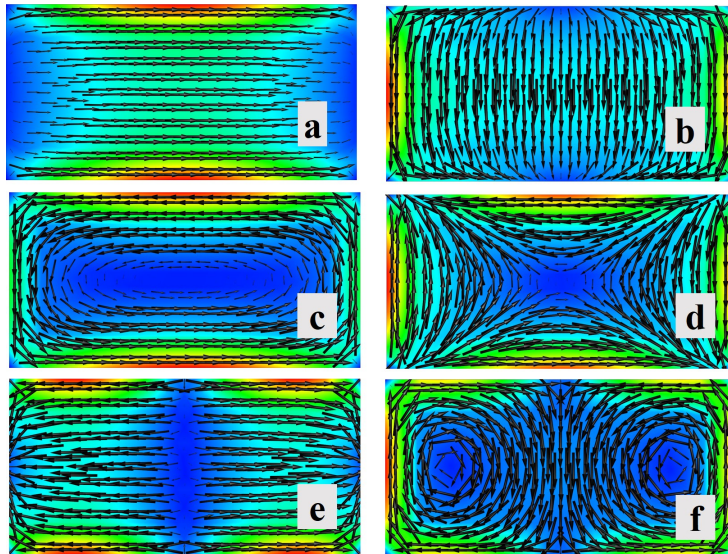

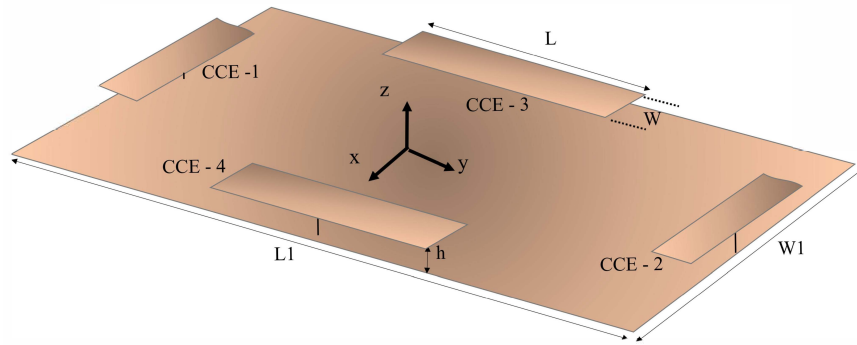**Figure 2**. Current distribution of a) mode 1, b) mode 2, c) mode 3, d) mode 4, e) mode 5, f) mode 6.

Figure 3. Complete structure.

Table 1. Effects of exciters on eigenvalues of the structure.

Mode number	Eigenvalue without exciters	Eigenvalue with exciters
Mode 1	0.415	0.501
Mode 2	−1.82	−0.723
Mode 3	5.28	5.11
Mode 4	−5.68	−2.01
Mode 5	−7.07	−5.546
Mode 6	29.8	22.32

3. Polynomial chaos expansion

Polynomial chaos expansion (PCE)-based surrogate model has been extensively implemented in statistical analysis of the antennas to alleviate the computational burden. In PCE, the main idea is to offer a polynomial surrogate for the computational model. In this sense, the polynomial expansion that relates the response of the system (Y) and the independent input parameters of M dimensional $\mathbf{X} = \{X_1, X_2, \ldots, X_M\}$ is given by:

$$Y = \sum_{\alpha \in N^M} y_\alpha \Psi_\alpha(\mathbf{X}) \tag{3}$$

where the $\Psi_\alpha(X)$ are the multivariate polynomials, α are the multiindices that indicate the degree of the polynomial in each of the input variables, and y_α are the unknown coefficients to be determined. The multivariate polynomials are constituted by the tensor products of the univariate orthogonal polynomials as:

$$\Psi_\alpha(\mathbf{x}) = \prod_{i=1}^{M} \Phi_{\alpha_i}^{(i)}(x_i) \tag{4}$$

where $\Phi_{\alpha_i}^{(i)}$ is the univariate orthogonal polynomial in the ith variable of degree α_i. The univariate orthogonal polynomials are chosen w.r.t. probability distribution of input parameters. Some commonly used classical univariate polynomials can be found in [17]. In order to implement the PCE, two primary methods become prominent: intrusive and nonintrusive methods. In intrusive methods, the underlying code of computational model is modified, which leads to a fast computation. However, it may not always be possible to modify the computational code and/or may need heavy calculations. On the other hand, nonintrusive methods handle the computational models as a black-box, i.e. no further adjustment on the code is needed, which makes it the more convenient choice. For that reason, nonintrusive method is preferred in this work. One of the methods to calculate the expansion coefficients nonintrusively is the least-square minimization. Since PCE provides an infinite polynomial series as shown in (3), it needs to be truncated to a finite sum for computational purposes, where truncation error exists. Then the least-square minimization can be set up. Moreover, the total polynomial basis P during the surrogate modeling can be computed with the permutation formula as (5):

$$P = \left(\frac{M + p}{p} \right) \tag{5}$$

where M refers to the total number of input parameters and p is the degree of the truncated polynomial expansion. Within the choice of the high polynomial degree due to the insurance of high accuracy surrogate

model and/or inevitable high number of input parameters, the number of polynomial bases dramatically increases, and it decreases the efficiency of the PCE. For that reason, two stepwise methods can be applied in PCE to only retain the basis functions that have the maximal effects on the response of the model. Since the high order polynomial interactions have the least effect on the model response, the hyperbolic truncation scheme, i.e. q-norm, is applied in PCE that has already been truncated with p-degree to avoid the interactions of higher order polynomials. Least angle regression method (LARS) is the second step to obtain the most effective polynomial bases [18]. Briefly, it is an iterative regression technique that starts with initializing all coefficients to zero, and setting the initial residual to the model response. Then, the predictor $\Psi(X)$, which has the highest correlation with the current residual is chosen. The coefficient of predictor moves in least-square sense until a predictor comes up with equal correlation with the first predictor. The algorithm continues until the P basis (also known as predictors) have been entered. At the end of the algorithm, the basis function that has the lowest leave-one-out error (error$_{LOO}$) are chosen among many possible basis functions set. One should keep in mind that the LARS algorithm is not applied to compute the expansion coefficients, but only the polynomials that have the largest impact on the model response are kept. Once a surrogate model is built, the error between the computational model and the surrogate one can be estimated. One possible option to evaluate the error is the normalized empirical error. It compares the resemblance of surrogate model results with the computational one. However, the empirical error leads to a well-known problem: overfitting. For that reason, leave-one-out cross validation error (error$_{LOO}$) is introduced for error calculation in PCE. The basic idea in calculating the error$_{LOO}$ is to build surrogate models by excluding one data set at each time. Then, a prediction is carried with the excluded data set on the built surrogate model. These predictions are carried on for each data set. Overall, the LARS and error$_{LOO}$ are together considered to obtain an accurate surrogate model. To obtain a more accurate surrogate model, i.e. if the error$_{LOO}$ does not reach a specified accuracy, new input samples are added, and the algorithm is repeated. The readers are encouraged to see the report [19] and the references therein for more detailed theoretical background of PCE.

4. Surrogate model

The structure under consideration has eight independent input parameters, namely the magnitude and phase of four CCE ports. The variation of input parameters is designated to have values between the allowable range, namely magnitude of each port is between [0, 1 V] and phase of each port is between $[-180^0, 180^0]$. Firstly, the input parameters are randomly sampled with 200 samples that are uniformly distributed. Since each input parameter has a uniform distribution, legendre orthogonal polynomials are chosen to obtain multivariate polynomial as stated in (4). The number of samples are increased until an accurate surrogate model is obtained, i.e. the error$_{LOO}$ reaches specified accuracy. In this work, the number of samples is increased to 1000 step by step to obtain a model that mimics the computational model very well. The numerical simulations are conducted with the computational model and the total normalized electric field is considered output for each input sample. Two outputs are taken into account for building two surrogate models, the radiation patterns regarding the elevation angles (the plane at $\phi = 90^0$) and the azimuth angles (the plane at $\theta = 90^0$). Once the computational simulations are accomplished, the obtained output and the corresponding input data are presented to PCE, and a surrogate model is built. In order to specify the degree of the polynomials, a degree-adaptive calculation is performed. By this way, the degree which yields the lowest error$_{LOO}$ can be automatically selected. Analogously, a q-norm adaptive truncation scheme is also applied. However, it is seen that both adaptive calculations decelerate the computation and bring computational burden. For that reason,

the q-norm value is set to be 0.7 and the degree is truncated at the $p = 11th$-order after a detail examination is performed on the results of adaptive calculation. Within the chosen values, the error $_{LOO}$ is ensured to be at minimum for both surrogate models. In this work, UQLab is used as a toolbox for all calculations and building the surrogate model [20].

In Figure 4a, seven elevation angles are chosen to explore the effect of increasing sample number on error $_{LOO}$. One can observe that the error $_{LOO}$ decreases to below 0.05 when the sample number is increased to 800 samples. The further increase of the sample number does not have great impact on the error. These findings are also observed for all elevation angles. On the other hand, for the surrogate model of the azimuth angles (see Figure 4b), the error $_{LOO}$ is decreased to 0.1 when the sample number reaches 800 and there are no significant decreases while further increasing the sample number. The same results are also verified for all azimuth angles. Consequently, either 800 or 1000 sample number is sufficient to obtain an accurate surrogate model for the investigated structure. One can keep in mind that further increasing the number of samples will bring a computational burden; hence, increasing the number of samples should be ended.
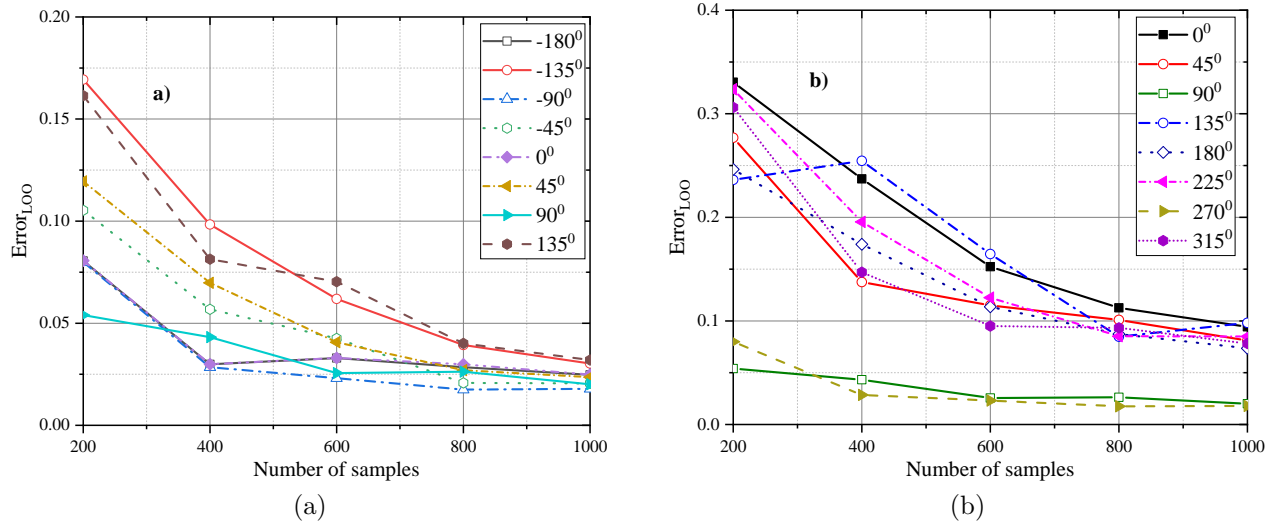

Figure 4. The $error_{LOO}$ vs. number of samples for different: a) elevation angles, b) azimuth angles.

In order to evaluate the performances of the obtained surrogate models, three test data, which are not used while building the surrogate models, are taken into consideration and the radiation patterns of computational model and the surrogate model are compared. Since the structure can exhibit similar performance for different input parameters, the test data are deliberately chosen to reveal the performance of the surrogate model for various radiation patterns. The values of test data are given in Table 2 (nominal values for each radiation case), and the comparisons are given in Figure 5. It can be observed that the surrogate model for the elevation angles demonstrates relatively the same radiation pattern in shape, but with reduced magnitudes for radiation case 1 (Figure 5a). It is believed that this mismatch is mainly due to the sampling process of the input parameters, which is uniformly distributed without applying any sampling technique for this study. In the literature, there exist special techniques such as latin hypercube sampling [19] and adaptive sampling process [21] to adequately sample the input parameters and then to reduce and optimize the input space. On the other hand, Figure 5b shows that the surrogate model for the azimuth angles of radiation case 1 exhibits close performance to the computational model. Moreover, the built surrogate models for radiation case 2 (Figures 5c and 5d) and

radiation case 3 (Figures 5e and 5f) offer relatively the same radiation patterns with the computational models for both elevation and azimuth angles.

Table 2. Excitation schemes for three radiation cases (m1: magnitude of port 1; p1: phase of port 1, etc.).

	Case 1 Nominal values	Case 1 Sampling range	Case 2 Nominal values	Case 2 Sampling range	Case 3 Nominal values	Case 3 Sampling range
m1 [V]	0.75	0.5 — 1	0.60	0.45 — 0.75	0.80	0.65 — 0.95
m2 [V]	0.75	0.5 — 1	0.70	0.55 — 0.85	0.30	0.15 — 0.45
m3 [V]	0.75	0.5 — 1	0.20	0.05 — 0.35	0.70	0.55 — 0.85
m4 [V]	0.75	0.5 — 1	0.60	0.45 — 0.75	0.60	0.45 — 0.75
p1 [degree]	0	-15 — 15	45	30 — 60	10	-5 — 25
p2 [degree]	0	-15 — 15	-90	-105 — -75	-130	-145 — -115
p3 [degree]	0	-15 — 15	90	75 — 105	-135	-150 — -120
p4 [degree]	0	-15 — 15	45	30 — 60	30	15 — 45

5. PCE-based sensitivity analysis

Once a surrogate model is built for a structure under consideration, it is straightforward to obtain the most influential input values on the output results. In this work, the most important parameters of excitation scheme, i.e. magnitude and phase parameters of the CCE ports are desired to obtain for different radiation patterns. Since a feeding network of four CCE ports for a desired pattern has to be implemented during the production process, identifying the most important input parameters for the corresponding radiation may ease the process of production. Sensitivity analysis can be very useful to handle these issues. Sensitivity analysis (SA) can expose the contribution of each input parameter of a computational model on its desired response. There are several methods that are well-established for sensitivity analysis on various kind of engineering problems [22, 23]. Among them, Sobol' decomposition [24] is chosen for SA in this work since the coefficient of the PCE to build the surrogate model is used without any further computation [25]. Sobol sensitivity analysis is basically the decomposition of the total output variance of the model into each variance of the input parameters. Hence, it is possible to deduce the most influential input parameters on the output results with the Sobol' indices. For more information on Sobol' indices, one can see the report [26], and the references therein.

For the sensitivity analysis, three total electric field patterns are taken into consideration to exhibit the influence of each port's magnitude and phase on the output. Three distinct radiation patterns with the nominal values of phase and magnitude of ports are examined with the uniformly distributed samples that are ranged as given in Table 2. The sensitivity analysis is carried out for both elevation and azimuth angles. The total Sobol' indices shown in Figure 6a state that the considered pattern is most sensitive to port 3 and port 4 for elevation angle while port 3 is the most influential parameter for azimuth angle. On the other hand, the magnitudes of each port does have similar effect on azimuth angle for case 2 while the port 4 has the most impact on the results as shown in 6b. Lastly, it can be seen from Figure 6c that the port 3 and port 4 are the most important parameters as in the case 1.

Within the obtained SA results, the complete structure is reconsidered in order to reduce the overall complexity of the design. For that purpose, according to the SA, the number of ports is reduced and the most influential parameters are kept with the conducting plate. Then, the nominal excitation schemes are applied to the ports that are kept on the conducting plate, and the output results are compared with the complete
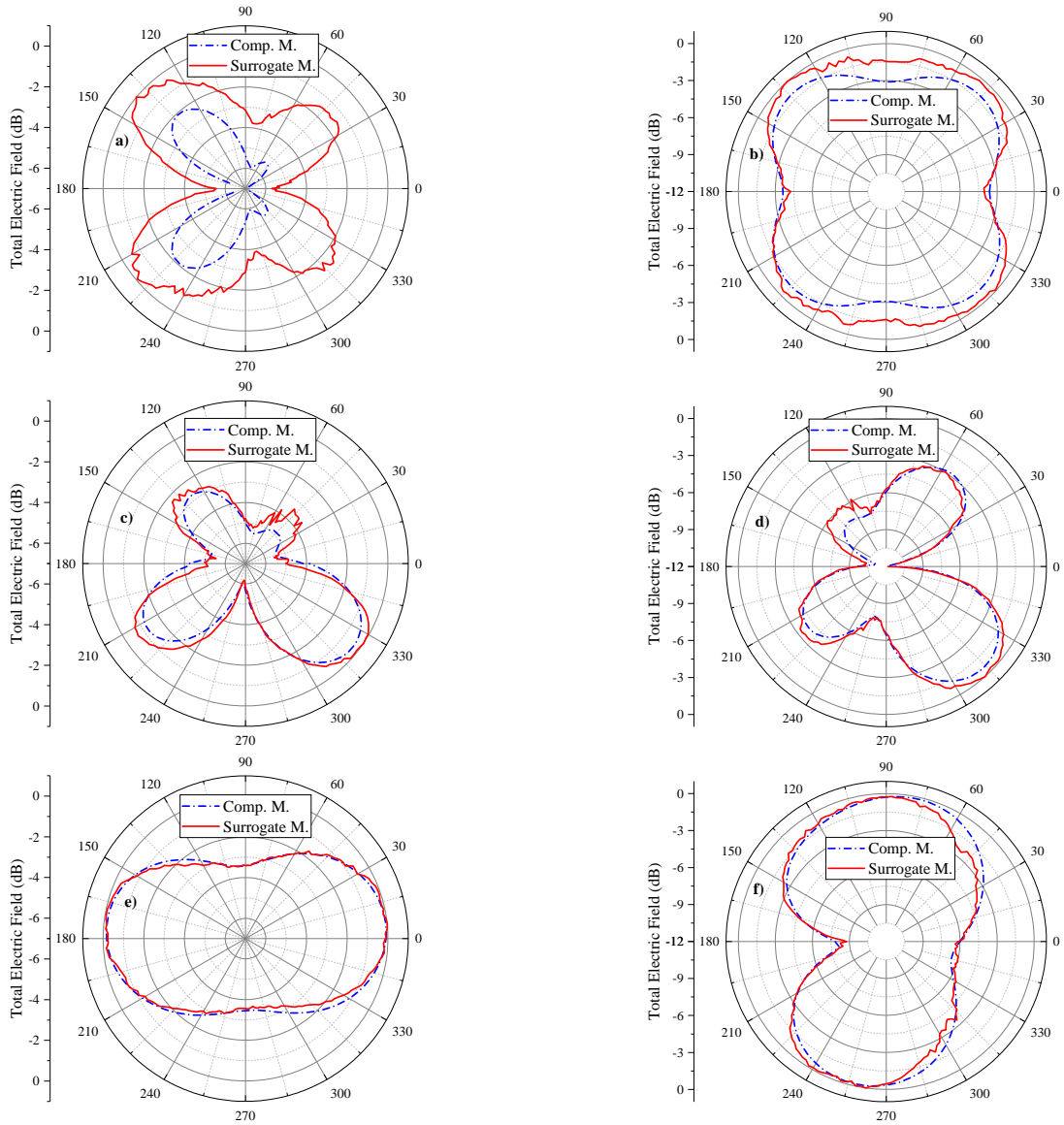
Figure 5. Comparison of the radiation patterns of surrogate model and computational model (each row corresponds to each radiation case, first column: $\phi = 90^0$ plane, second column: $\theta = 90^0$ plane).
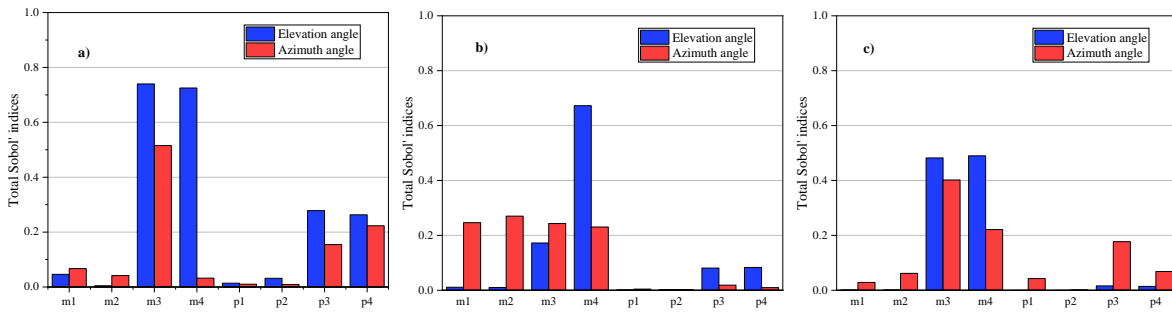

Figure 6. Total Sobol' indices of each input variable for: a) case 1, b) case 2, c) case 3.

structure, i.e. structure with four ports. For case 1 and 3, only port 3 and port 4 are kept with the structure, and it can be deduced that by comparing the corresponding radiation patterns, the antenna with reduced ports exhibits close performance to the antenna with four port design for case 1 (Figures 7a and 7b). On the other hand, the reduction of ports does not satisfy adequate performance for case 2 (Figures 7c and 7d). This mismatch is expected since the results of the SA (see Figure 6b) indicates that all magnitudes of ports are equally important for the considered radiation pattern. The same conclusion for case 1 is also obtained for case 3 (Figures 7e and 7f). In addition, the correlation between the patterns for four ports and two ports designs are also numerically compared and listed in Table 3.
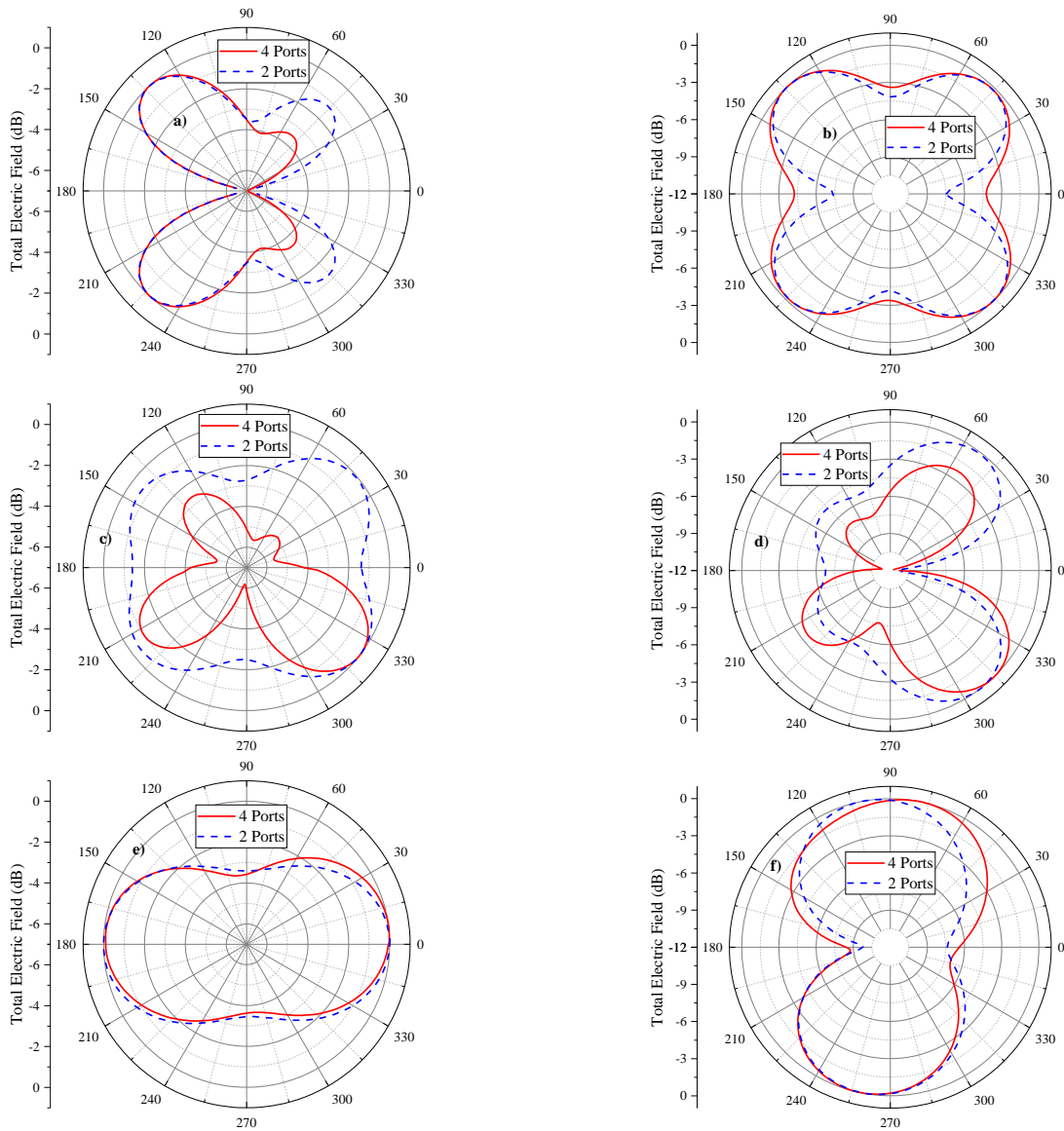

Figure 7. Comparison of the radiation patterns of two different designs: 4 ports and 2 ports (each row corresponds to each radiation case, first column: $\phi = 90^0$ plane, second column: $\theta = 90^0$ plane (all results are in dB)).

Table 3. Correlations between the radiation patterns of structures with four ports and two ports

	Case 1	Case 2	Case 3
$\phi = 90^0$	0.9902	0.5196	0.9839
$\theta = 90^0$	0.9756	0.7968	0.9482

6. Conclusion

A procedure for building a surrogate model for a perfect electric conductor with four coupling element is proposed. The radiation pattern of the structure is investigated, and the location of the coupling elements are decided with the help of characteristic mode analysis. Two surrogate models regarding the elevation and the azimuth angles are built to avoid the numerical complexity of the complete structure. An error analysis is presented to demonstrate the similarity between the computational model and the surrogate one. A sensitivity analysis is conducted to determine the most influential input parameters on the radiation patterns. These results help to reduce the number of ports; hence, decreases the complexity of the structure for a desired radiation pattern. More complex computational model may be considered with the proposed method, which remains as a future work.

References

[1] Ma R, Shih TY, Lian R, Behdad N. Design of bandwidth-enhanced platform-mounted electrically small VHF antennas using the characteristic-mode theory. IEEE Antennas and Wireless Propagation Letters 2018; 17 (12): 2384-8.

[2] Castillo RF, Ma R, Behdad N. Platform-Based, Electrically-Small HF Antenna With Switchable Directional Radiation Patterns. IEEE Transactions on Antennas and Propagation. 2021; 69 (8): 4370-9.

[3] Chen Y, Wang CF. HF band shipboard antenna design using characteristic modes. IEEE Transactions on Antennas and Propagation 2015; 63 (3): 1004-13.

[4] Chen Y, Wang CF. Electrically small UAV antenna design using characteristic modes. IEEE Transactions on Antennas and Propagation 2013; 62 (2): 535-45.

[5] Garbacz R, Turpin R. A generalized expansion for radiated and scattered fields. IEEE transactions on Antennas and Propagation 1971; 19 (3): 348-58.

[6] Harrington R, Mautz J. Theory of characteristic modes for conducting bodies. IEEE Transactions on Antennas and Propagation 1971; 19 (5): 622-8.

[7] Martens R, Manteuffel D. Systematic design method of a mobile multiple antenna system using the theory of characteristic modes. IET Microwaves, Antennas & Propagation 2014; 8 (12): 887-93.

[8] Robert CP, Casella G, Casella G. Monte Carlo statistical methods. New York, USA: Springer, 2004.

[9] Sudret B. Uncertainty propagation and sensitivity analysis in mechanical models–Contributions to structural reliability and stochastic spectral methods. Habilitationa diriger des recherches, Université Blaise Pascal, Clermont-Ferrand, France 2007.

[10] Zou R, Lung WS, Wu J. An adaptive neural network embedded genetic algorithm approach for inverse water quality modeling. Water Resources Research 2007; 43 (8): 1-13.

[11] Kleijnen JP. Kriging metamodeling in simulation: A review. European journal of operational research 2009; 192 (3): 707-16.

[12] Zhang X, Srinivasan R, Van Liew M. Approximating SWAT model using artificial neural network and support vector machine. JAWRA Journal of the American Water Resources Association 2009; 45 (2): 460-74.

[13] Boeykens F, Rogier H, Vallozzi L. An efficient technique based on polynomial chaos to model the uncertainty in the resonance frequency of textile antennas due to bending. IEEE Transactions on Antennas and Propagation 2013; 62 (3): 1253-60.

[14] Acikgoz H, Mittra R. Stochastic polynomial chaos expansion analysis of a split-ring resonator at terahertz frequencies. IEEE Transactions on Antennas and Propagation 2018; 66 (4): 2131-4.

[15] Acikgoz H, Arya RK, Wiart J, Mittra R. Statistical electromagnetics for antennas. In: Developments in Antenna Analysis and Design: Volume 2. 1st ed. Institution of Engineering and Technology 2018; 259–286.

[16] Kishor KK, Hum SV. A two-port chassis-mode MIMO antenna. IEEE Antennas and Wireless Propagation Letters 2013; 12: 690-3.

[17] Xiu D, Karniadakis GE. The Wiener–Askey polynomial chaos for stochastic differential equations. SIAM journal on scientific computing. 2002; 24 (2): 619-44.

[18] Blatman G, Sudret B. Adaptive sparse polynomial chaos expansion based on least angle regression. Journal of computational Physics 2011; 230 (6): 2345-67.

[19] Marelli S, Sudret B. UQLab user manual – Polynomial chaos expansions, Report #UQLab-V1.3-104, Chair of Risk, Safety and Uncertainty Quantification, ETH Zurich, Switzerland, 2019.

[20] Sudret B, Marelli S. UQLab: A Framework for Uncertainty Quantification in MATLAB, In: The 2nd International Conference on Vulnerability and Risk Analysis and Management, University of Liverpool, United Kingdom 2014; 2554–2563.

[21] Acikgoz H, Santandréa L, Le Bihan Y, Gyimóthy S, Pavo J et al. Generation and use of optimised databases in microwave characterisation. IET Science, Measurement & Technology 2008; 2 (6): 467-73.

[22] Helton JC, Johnson JD, Sallaberry CJ, Storlie CB. Survey of sampling-based methods for uncertainty and sensitivity analysis. Reliability Engineering & System Safety 2006; 91 (10-11): 1175-209.

[23] Borgonovo E, Plischke E. Sensitivity analysis: a review of recent advances. European Journal of Operational Research 2016; 248 (3): 869-87.

[24] Sobol IM. Global sensitivity indices for nonlinear mathematical models and their Monte Carlo estimates. Mathematics and computers in simulation 2001; 55 (1-3): 271-80.

[25] Sudret B. Global sensitivity analysis using polynomial chaos expansions. Reliability engineering & system safety 2008; 93 (7): 964-79.

[26] Marelli S, Lamas C, Konakli K, Mylonas C, Wiederkehr P et al. UQLab user manual – Sensitivity analysis, Report #UQLab-V1.3-106, Chair of Risk, Safety and Uncertainty Quantification, ETH Zurich, Switzerland, 2019.